IX CONGRESSO BRASILEIRO DE
ENGENHARIA E CIÊNCIAS TÉRMICAS

9th BRAZILIAN CONGRESS OF THERMAL
ENGINEERING AND SCIENCES

Paper CIT02-0776

MEASUREMENT OF RADIATIVE HEAT FLUX IN NON-CONVENTIONAL GEOMETRIES AND COMPARISON WITH MODELING TECHNIQUES

José Sérgio de Almeida
Instituto Nacional de Pesquisas Espaciais, Laboratório de Integração e Testes, 12227-010 – São José dos Campos, SP - Brazil
jsergio@lit.inpe.br

Abstract. *A new methodology, based on the Discrete Ordinates Method (DOM), was developed to analyze thermal radiation in complex geometries. Reducing the angular dependence of the thermal radiation in a number of discretized directions, information is carried from the thermal conditions and thermo-optical properties of the surfaces under study. Approximating the solution of the Equation of Transfer by iteration, heat transfer functions can be predicted at the walls and in the interior of analytical cells from a test system. An experimental set-up was built, including a number of internal boxes with arbitrary specification of size, shape and layout, simulating spacecraft subsystems undergoing a technical situation of a thermal vacuum test. Varying the thermal conditioning of the walls and the boxes, radiative heat flux could be produced and were measured. Taking the necessary precautions in terms of identifying and properly compensating the differences of the thermo-optical properties and the temperature between the surfaces of the radiometer and the test system, a very good correlation was obtained between the numerical thermal modeling and the laboratorial measurements, in this way simultaneously validating the proposed mathematical approximation by using the DOM and the experimental methodology for the measurement of the radiative heat flux.*

Keywords*. Thermal Radiation, Heat Flux, Discrete Ordinates Method, Spacecraft Testing*

1. Introduction

Ground-based thermal vacuum tests of spacecraft are performed in order to verify the proper operation of the subsystems and the system as a whole when submitted and exposed to the extremes of vacuum and high and low temperature conditioning. Installed inside a large vacuum chamber, the space artefact is thermally isolated from the structures but properly submitted to the thermal loads from the solar and earth radiation, and the heat sinks of the cold space. Considering the typical uneven shape of actual spacecraft, the incoming and the internal generated thermal radiation is internally propagated in a multi-form of emission, absorption and reflection by all its thermally participating surfaces. A local flux conditioning in a particular part of the spacecraft will then be a result of this entire phenomenon.

The analysis of the resultant thermal radiation in a complex geometry situation like this is not straightforward. One of the alternatives is to search for mathematical approximating methods that can give acceptable results.

In the past few years some authors have been presenting and suggesting the applicability of the Discrete Ordinates Method for the analysis of thermal radiation in enclosures. The main purpose of this work is to develop a DOM-based mathematical modeling for thermal radiative heat transfer analysis and heat flux prediction inside non-conventional geometries completed with an experimental test set-up capable of performing surface radiative heat flux measurements. A satisfactory result from the comparison of the experimental results of the thermal radiation phenomenon inside more complex geometries with the computational predictions will qualify both the experimental technique and the mathematical approach. The data presented in this paper shows that this goal was successfully achieved.

2. The mathematical modeling approach

In enclosures holding non-conventional geometries, the occurrence of multi-emission and multi-reflection of thermal radiation from the many participating surfaces makes the radiative transfer analysis as extremely demanding. The analytical solution of the radiative heat flux taking place in such complex geometries is very difficult if not impossible to be obtained (Corlett, 1966; Crosbie and Schenker, 1982; Selçuk and Kayakol, 1997). A numerical approximation based on the Discrete Ordinates Method has been developed and presented by the heat transfer community (Chandrasekhar, 1960; Lee, 1962; Carlson and Lathrop, 1968; Fiveland, 1984, 1988; Truelove, 1987), and it is now used here with an enhanced and improved formulation to predict net heat flux values on the surfaces of a real 3-Dimensional enclosure including non-conventional internal geometries. Based on the Equation of Transfer, the approach for an absorbing, emitting and non-scattering intervening gray medium can be expressed as (Modest, 1993).

$$\frac{dI}{ds} = \hat{\mathbf{s}} \cdot \nabla I(\mathbf{r}, \hat{\mathbf{s}}) = \kappa(\mathbf{r}) I_{\mathrm{b}}(\mathbf{r}) - \kappa(\mathbf{r}) I(\mathbf{r}, \hat{\mathbf{s}}) \tag{1}$$

For the enclosure internal walls, Eq. (1) is subjected to the radiative boundary conditions:

$$I(\mathbf{r}_w,\hat{\mathbf{s}}) = \varepsilon(\mathbf{r}_w)\, I_b(\mathbf{r}_w) + \frac{\rho(\mathbf{r}_w)}{\pi}\int_{\hat{\mathbf{n}}\hat{\mathbf{s}}<0} I(\mathbf{r}_w,\hat{\mathbf{s}}')\,|\hat{\mathbf{n}}\cdot\hat{\mathbf{s}}|\,d\Omega' \tag{2}$$

which expresses the surface outgoing intensity of radiation, considered as a sum of the emitted intensity as a consequence of the temperature of the boundary surface, and the reflected portion of the incoming radiative intensity. In using the Discrete Ordinates Method, the physical enclosure under study is considered as the computational domain, which is then appropriately divided into many relatively small control volumes, or cells. For each one of these cells, Eqs. (1) and (2) are applied and solved for a set of *n* discrete and distinct directions (i = 1, 2,..., n), and the integrals that represent the angular functions are approximated by numerical quadrature, with the associated quadrature weights representing areas on the unit sphere around a cell-centered point *P*. The finite-difference form of Eq.(1) can be integrated over the six surfaces of the control volume and, after relating the radiation conditions of the downstream surfaces to the upstream surfaces using a technique called linear weighting differencing scheme which is here represented by the factor γ, the estimation of the cell-center averaged radiative intensity for the control volume is then given by (Modest, 1993)

$$I_{pi} = \frac{\kappa V\gamma S_{pi} + |\xi_i| A_{XR} I_{XRi} + |\eta_i| A_{YR} I_{YRi} + |\mu_i| A_{ZR} I_{ZRi}}{\kappa V\gamma + |\xi_i| A_{XR} + |\eta_i| A_{YR} + |\mu_i| A_{ZR}} \tag{3}$$

where A_{XR} and I_{XR} are respectively the area and the local average value of radiant intensity, at the face of the volume element, in this particular case perpendicular to the *x*-direction (see Fig. 1).

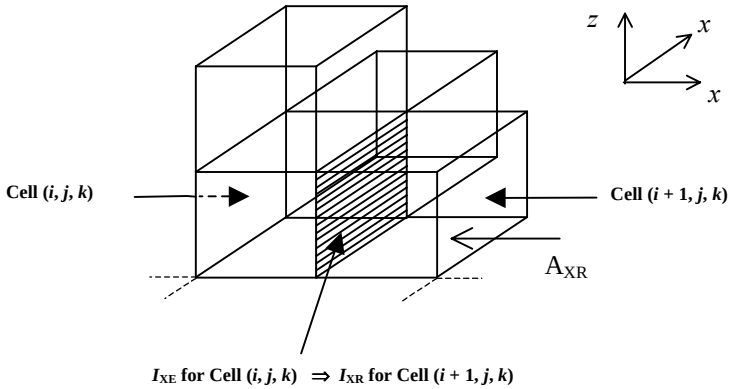

Figure 1. The process of downstreaming the cell intensity

Based on approach by Patankar (1980), Sanchez and Smith (1992) and Chai *et al* (1993) for non-conventional geometries including protrusion walls, we modify Eq. (3) by adding two terms in order to deal with the new internal boundary conditions. This will lead to

$$I_{pi} = \frac{\kappa V\gamma S_{pi} + |\xi_i| A_{XR} I_{XRi} + |\eta_i| A_{YR} I_{YRi} + |\mu_i| A_{ZR} I_{ZRi} + R_C V\gamma}{\kappa V\gamma + |\xi_i| A_{XR} + |\eta_i| A_{YR} + |\mu_i| A_{ZR} - R_p V\gamma} \tag{4}$$

where, for the protrusion surfaces it must be considered

$$R_{C\,x} = \frac{1}{dx\,\gamma}\left[\varepsilon_w\, I_{bw} + \frac{1-\varepsilon_w}{\pi}\sum_{\xi_i<0}\omega_j\, I_{w\,j}\,|\xi_j|\right] \tag{5}$$

$$R_{P\,x} = 0$$

In addition, inside the protrusions we have to set

$$R_C = 0$$
$$R_P = M$$
$$\gamma = 1.0$$

where to M is assigned a relatively large number.

In an iterative way, Eq.(4) is then used to approximate the intensity of radiation in every single control volume of the spatial domain, leading to the calculation of the radiative heat flux taking place at the enclosure internal walls.

3. The experimental set-up

In order to perform the experimental measurements of radiative heat flux in non-conventional geometries, it was designed and built a full size metallic enclosure containing three boxes closely simulating the thermal behavior of operating spacecraft subsystems. These internal boxes hold distinct characteristics of shape, dimension, thermo-optical properties and lay-out, and they are individually thermally conditioned and controlled to distinct temperatures. For the generation of the radiative heat fluxes in the experiment, the boxes, thermally insulated from the enclosure walls and considered as opaque for the thermal radiation, were defined to be heated up while the enclosure walls would be maintained at lower values of temperature. In this way, the resultant multi-reflected-emitted radiative heat flux values could be measured at the enclosure cold walls. All the active surfaces are considered to have gray thermo-optical properties. This basic but realistic test system was designed to approach the mathematical thermal modeling of the environmental conditions to be reproduced by the analytical computer software. Figure 2 presents the geometry of the proposed test system and in Tab. (1) it can be found its dimensional and lay-out details.

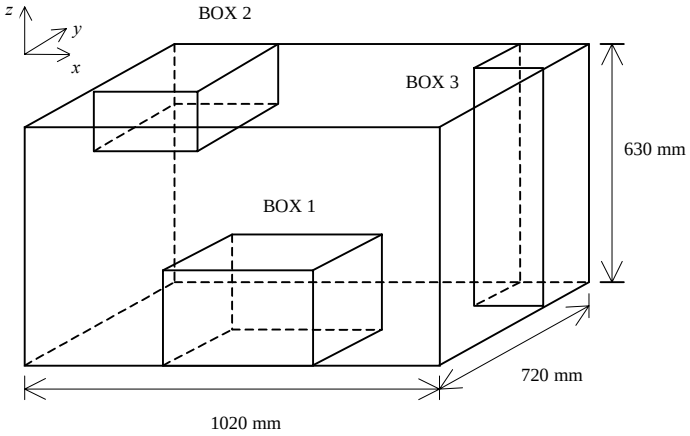

Figure 2. Proposed configuration for this analysis of thermal radiation in 3-D non-conventional geometries

For the monitoring of the test system thermal conditioning, approximately eighty temperature sensors are installed on the enclosure and boxes active surfaces, and the average of their readings are used to set the conditions for each test case under analysis.

Table 1. Geometrical specification for the proposed 3-D test configuration as presented in Figure 2

		Dimension [mm]	**Number of cells**	**Position (cell no.)**
Enclosure	*x*-axis:	1020	34	-
	y-axis:	720	24	-
	z-axis:	630	21	-
Box 1	*x*-axis:	360	12	$13 \rightarrow 24$
	y-axis:	300	10	$1 \rightarrow 10$
	z-axis:	240	8	$1 \rightarrow 8$
Box 2	*x*-axis:	240	8	$1 \rightarrow 8$
	y-axis:	480	16	$9 \rightarrow 24$
	z-axis:	120	4	$18 \rightarrow 21$
Box 3	*x*-axis:	210	7	$28 \rightarrow 34$
	y-axis	210	7	$18 \rightarrow 24$
	z-axis	630	21	$1 \rightarrow 21$

For the measurement of the resultant radiative heat fluxes, horizontal strips containing surface measurement cells are selected on the enclosure walls as can be seen in Fig. 3. The radiative heat flux sensors, custom-made at the same size of a modeling cell (30mm x 30mm), are attached flush to the surface in order to produce the desired readings. Since the test enclosure is filled with air, the analysis of radiative heat transfer can be considered as in radiatively non-participating medium (Siegel and Howell, 1992; Brewster, 1992). This is carried out by assigning in the numerical modeling the absorption coefficient κ a very small value.

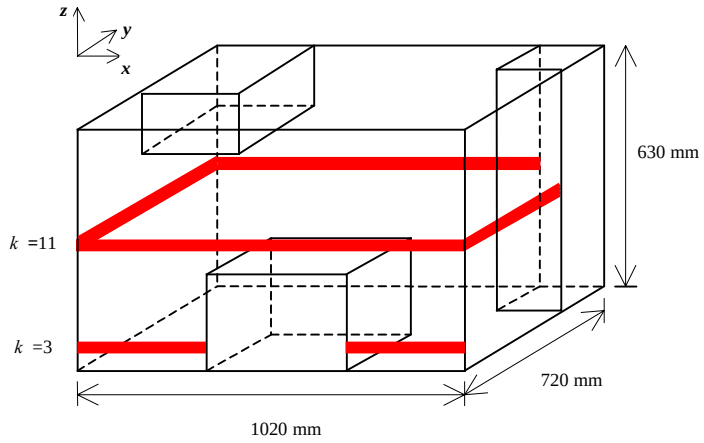

Figure 3. Wall horizontal strips containing the cells for the heat flux readings

4. The proposed approach for the radiative heat flux measurements

The proper and accurate measurement of net radiative heat flux taking place in the walls of a 3-Dimensional thermal system depends on some operational considerations. In principle, the simple act of positioning a sensor with a significant area on top of a surface will immediately modify the conditions of net radiative heat flux taking place in that particular surface without the sensor. The only situation where virtually no changes take place is when the sensor is maintained at the same temperature of the surface where it is installed and, at the same time, the sensor surface holds the same thermo-optical properties of the original wall surface. When distinct wall-radiometer surface characteristics are present, some kind of correction must be performed and this can be called a *thermo-optical compensation*.

In addition, considering the possibility that at the moment of the measurement of heat flux, the sensor surface temperature is not necessarily exactly the same as the original surface, a second correction must be made in order to get the desired values as for the condition when no radiometer is installed on the original surface. This case is then called *temperature compensation*. This physical situation can be visualized in Fig. 4.

a) original configuration b) with the radiometer installed

Figure 4. Analysis of net heat flux taking place on the measuring cell

In order to calculate the net heat flux for both situations, we use the equation that express the net radiative heat flux experienced by a gray surface (Modest, 1993).

$$q_i = \varepsilon_i \sigma T_i^4 - \alpha_i H_i \qquad (6)$$

To calculate the desired value of radiative heat flux on the wall, q_w, we can now observe that, if the size of the radiometer is relatively very small when compared to all the other radiatively participating walls on the surroundings, as happens in the situation of this experiment, variations in the radiometer surface temperature and optical properties will not significantly affect the incoming radiation H_w, because the new value of radiosity leaving the radiometer surface is not able to cause a representative impact on the heat balance of the system as a whole.

Therefore, following this approximation of

$$H_s \approx H_w \tag{7}$$

We will then have that

$$H_s = \sigma T_s^4 - \frac{q_s}{\varepsilon_s} \tag{8}$$

and

$$q_w = \varepsilon_w \sigma T_w^4 - \varepsilon_w \left(\sigma T_s^4 - \frac{q_s}{\varepsilon_s} \right) \tag{9}$$

and finally

$$q_w = \varepsilon_w \sigma \left(T_w^4 - T_s^4 \right) + \frac{\varepsilon_w}{\varepsilon_s} q_s \tag{10}$$

Equation (10) is able to convert the measurement results of radiative heat flux taking place on the radiometer surface to the expected value for the actual enclosure wall and in so doing, simultaneously compensating for both the thermo-optical and the temperature differences.

To perform the radiative heat flux measurements, a special kind of sensor was used (Captec, 1999) which is designed to strongly minimizing the effects of convective heat transfer. Custom made for this experiment, this planar type of sensor is constructed using alternated parallel strips of highly absorptive material (Kapton) and highly reflective material (Aluminum). From the impinging thermal radiation on top of the active sensor area, a number of thermocouples installed underneath of the Kapton material will read relatively higher values of temperature, while thermocouples located under the Aluminum strip will read relatively lower values of temperature. This thermopile arrangement will produce a voltage that is proportional to the net heat flux experienced by the sensor.

A simple diagram showing this principle of operation is presented in Fig. 5.

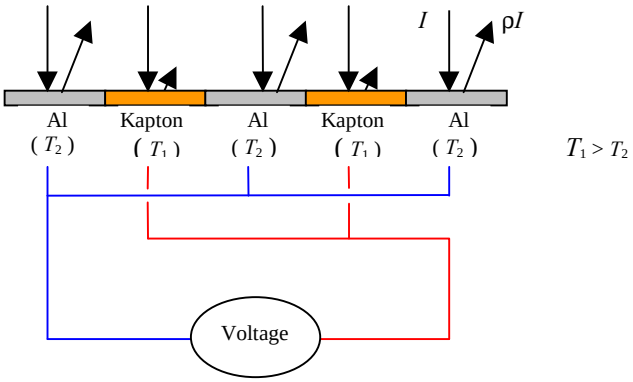

Figure 5. Functional diagram of the planar radiometer (Captec, 1999)

For this work, the radiometer was adequately calibrated using four values of target temperature namely 35°C, 65°C, 95°C and 125°C (Almeida, 2000) which fully covered the range of radiative heat flux to be measured in the experiment.

5. Experimental results and comparison with the computational prediction

In order to verify and compare the performance and accuracy of the proposed thermal modeling and the laboratorial measurements approaches for this radiative heat transfer study, a number of test cases were developed (Almeida, 2000). These included several distinct conditions of box temperature, lay-out and surface thermo-optical properties. For the DOM mathematical modeling, a S_{16} order of approximation was adopted representing a discretization of the intensity of radiation in the unit sphere in 288 distinct directions. This selected order of approximation proved to be more accurate when compared with lower orders of the numerical method, for this particular application.

From the study, three selected test cases are now presented.

Test Case 1: The first test case considers the analysis of net heat flux taking place on the horizontal strip that include the 3rd cells of the z-axis, enclosure surface where $y = 0$, for the subsystem positions as represented in Fig. (2). The settings for the thermal condition can be seen in Tab. (2) and the average measured temperature for the enclosure and box surfaces are presented in Tab. (3). These values of temperature together with the surface thermo-optical conditions are taken to the DOM-based computer numerical modeling in order to predict the radiative heat flux on the enclosure walls. For a visual comparison, these results are taken to Fig. (6) together with the data obtained from the laboratorial heat flux measurements.

Table 2. Set-up conditions for Test Case 1

TEST CASE	**1**	
BOXES POSITION	As shown in Figure 2 and detailed in Table 1	
BOX & ENCLOSURE SURFACES CONDITION	All covered with Kapton® tape, ε = 0.846	
BOXES TEMPERATURE	Box 1	130ºC
	Box 2	90ºC
	Box 3	50ºC

Table 3. Experimental averaged temperature recorded during Test Case 1

BOX 1		**BOX 2**		**BOX 3**	
130.9ºC		91.9ºC		50.9ºC	
ENCLOSURE WALLS					
$x = 0$	$x = 1020$mm	$y = 0$	$y = 720$mm	$z = 0$	$z = 630$mm
22.0ºC	18.6ºC	22.9ºC	20.6ºC	18.6ºC	23.5ºC

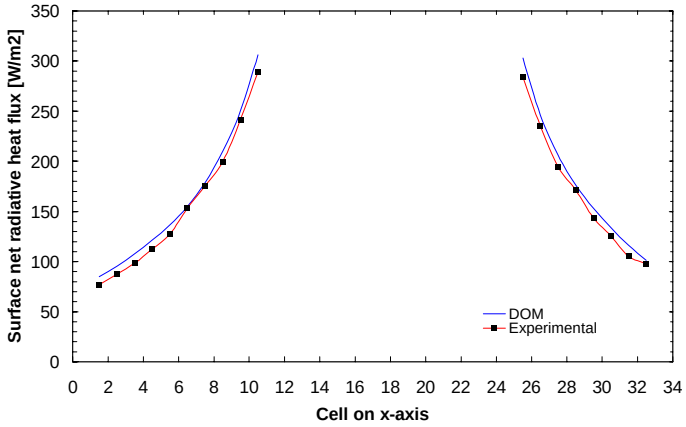

Figure 6. Comparative results from Test Case 1

For this first comparison of predicted and experimental data, in this particular case analyzed in a region located in the lower part of the enclosure surface where $y = 0$, it can be seen in Fig. (6) that for both enclosure sides related to the position of Box 1 the results are in very good agreement, perfectly following the trend of producing higher values of radiative heat flux as the position of the measurement cell approaches the lateral surfaces of Box 1. Analyzing the data, it was found that the average (arithmetic mean) in the difference between both modeling prediction and experimental data is 6.1 % with the highest single value of difference being 10.7 %. The standard deviation was calculated and found to be 2.8 %.

Recalling that these results of radiative heat flux, predicted and measured in a number of cells located on the enclosure wall (for this particular test case a number of 18 distinct cells) are a consequence of the phenomenon of multi-emitting, reflecting and absorbing thermal radiation throughout the active surfaces of this radiatively accounted complex geometry, these obtained values of difference and standard deviation can be considered as very good.

Test Case 2: This second test considers a significant change in the surface temperature of the internal boxes. The adopted strategy was to swap the assigned temperature value of the boxes in a kind of clockwise rotation, looking in a top view of Fig. (2) for instance. The new specifications for the box temperature can be seen in Tab. (4).

As can be seen in this table, Box 2 now has the highest temperature while Box 1 has the lowest value. This imposes a different level of radiative heat flux on the enclosure walls.

In terms of the radiative heat flux reading positions on the enclosure walls, these are now to occur on the horizontal strips as shown in Fig. (3), for the surface where x = 1020mm, and for the centered level at k = 11.

Table 4. Set-up conditions for Test Case 2

TEST CASE	**2**	
BOXES POSITION	As shown in Figure 2 and detailed in Table 1	
BOX & ENCLOSURE SURFACES CONDITION	All covered with Kapton® tape, ε = 0.846	
BOXES TEMPERATURE	Box 1	50ºC
	Box 2	130ºC
	Box 3	90ºC

For this Test Case 2, the thermal conditions in terms of surface temperature recorded during the test were as presented in Tab. (5).

Table 5. Experimental averaged temperature recorded during Test Case 2

BOX 1		**BOX 2**		**BOX 3**	
51.3ºC		132.1ºC		91.1ºC	
ENCLOSURE WALLS					
x = 0	x = 1020mm	y = 0	y = 720mm	z = 0	z = 630mm
19.2ºC	16.6ºC	16.7ºC	17.8ºC	15.8ºC	21.6ºC

Performing the heat flux evaluation with its required thermo-optical compensation calculation and the numerical prediction using the Discrete Ordinates Method, the results are graphically presented in Fig. (7).

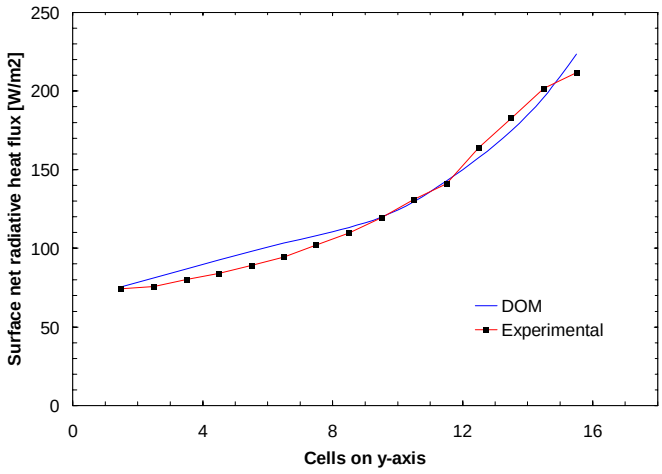

Figure 7. Comparative results from Test Case 2

For this comparison of radiative heat flux taking place at the enclosure wall where x = 1020mm as presented in Fig. (7), the average value for the difference between the predicted and the practical data was 3.4 % and the standard deviation, 5.1 %. For these curves, the highest single value of difference was found to be 10.1%.

Test Case 3: For Test Case 3, two further distinct modifications were proposed in order to verify the correlation of both mathematical modeling and experimental measurements: a box lay-out modification and a surface thermo-optical property differentiation. For the new lay-out assignment, Box 1 was physically moved from its original place to a position attached to the enclosure corner where x = 1020mm and y = 0.

Box temperatures are maintained according to Tab. (4). This new geometrical condition tests the capability of the theoretical modeling to cope with a change in a radiative heat source position internally to the experimental set-up so as to determine whether the resultant values of radiative heat flux taking place on the enclosure walls can be predicted with accepted accuracy. For the surface thermal optical property differentiation, part of the enclosure surface where the heat flux is intended to be measured was actually covered with a selected kind of tape producing a much distinct thermo-optical characteristic. This will allow the test to verify the sensitivity of this parameter in the system.

Table 6. Set-up conditions for Test Case 3. Box 1 new lay-out and details of the reflective tape application

TEST CASE		**3**		
Box 1 new lay-out				
		Dimension [mm]	Number of cells	Position (cell no.)
Box 1	x-axis:	360	12	23 → 34
	y-axis:	300	10	1 → 10
	z-axis:	240	8	1 → 8
Highly Reflective Aluminum Tape Installation (ε = 0.029)				
Box 2	- Box 2 face at y = 240 mm - Dimension: 120 mm x 240 mm			
Enclosure surface x = 1020 mm	- in y-axis: from y = 300 mm to 510 mm - in z-axis: from z = 210 mm to 420 mm - Dimension: 210 mm x 210 mm			

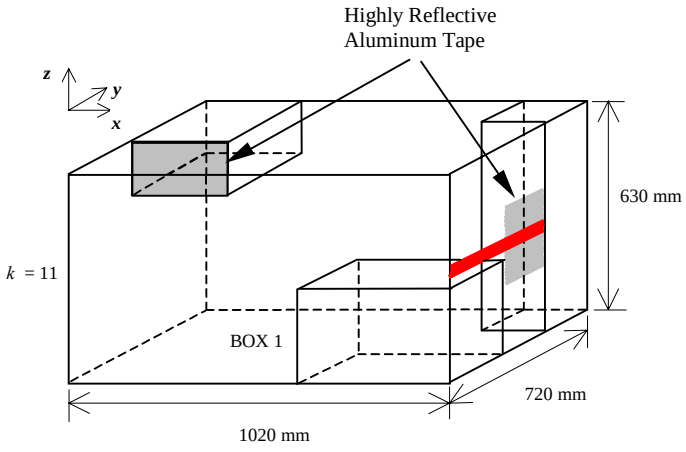

Figure 8. New box lay-out and differentiate thermo-optical properties on part of the test surface

Figure 8 shows the proposed new physical location of Box 1 in the experiment and also the assignment of the new optical properties of Box 2 and at the enclosure surface where x = 1020mm. Table 6 presents the coordinates in terms of cell number related to this new positioning and also the details of the new properties for part of the enclosure and Box 2 surfaces.

Table 7. Experimental averaged temperature recorded during Test Case 3

BOX 1		**BOX 2**		**BOX 3**	
51.5ºC		131.7ºC		91.1ºC	
ENCLOSURE WALLS					
$x = 0$	$x = 1020$ mm	$y = 0$	$y = 720$ mm	$z = 0$	$z = 630$ mm
17.9ºC	15.5ºC	15.2ºC	16.9ºC	14.8ºC	20.6ºC

For this test case, it can be observed from Fig. (9) that the results obtained from the experimental measurements follow acceptably well the theoretical predictions of radiative heat flux for these new circumstances.

Comparing with Fig. (7), which presents results for the situation where Box 1 was in its original position, Fig. (9) clearly shows now the resultant increase in the enclosure wall net heat flux for those cells located at lower values of y.

Also in Fig. (9), it is possible to note the large decrease of the enclosure wall heat flux when passing from the highly absorptive (Kapton tape, $\alpha = 0.846$) to the highly reflective surface cells (Aluminum tape, $\alpha = 0.029$). It can be seen that there is a close agreement between the numerically predicted and the experimental measurement results with this sudden variation on the enclosure wall net heat flux.

For this 3rd test, the average value for the difference between the theoretical and practical results was found to be 1.5 % with the standard deviation calculated as 3.6 %. For these curves, the highest single difference value was 6.0 %.

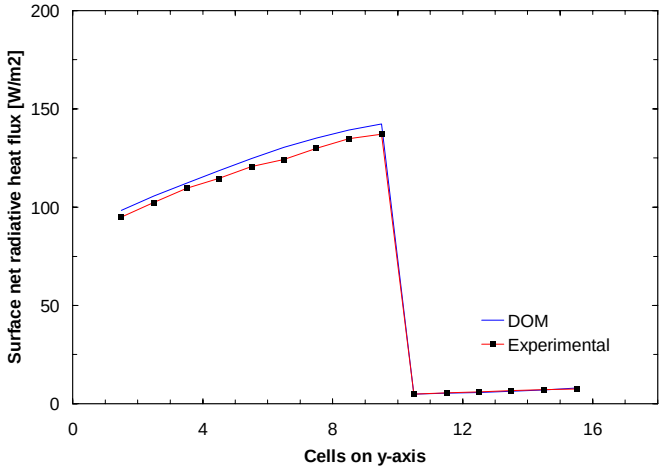

Figure 9. Comparative results from Test Case 3

6. Conclusion

A new formulation based on the Discrete Ordinates Method had been developed and it is now here concisely presented. This computational numerical approximation was designed to be capable of handling radiative heat flux analysis in 3-Dimensional enclosures containing a significant extent of geometrical and thermo-optical non-conventional configuration. This physical situation approaches the operational characteristics of real thermal systems in terms of the presence of multi-emission, absorption and reflection of thermal radiation, in virtually all directions.

In parallel, an experimental test set-up incorporating the circumstances of the thermo-optical and geometrical proposed configuration was designed and built with the objective of performing measurements of the resultant radiative heat flux on the enclosure walls. Comparing both the theoretical data with the experimental results it was found that, if the necessary precautions are taken in terms of proper surface thermo-optical and temperature compensation for the heat flux measurements, a very good correlation between the mathematical thermal modeling and the experimental measurements can be obtained.

7. Acknowledgment

The author would like to thank Dr. W. Malalasekera and Dr. H. James from Loughborough University, UK, for their supervision and guidance on the original work, the Brazilian institution CAPES for the financial support and also the National Institute for Space Research – INPE for its valuable cooperation.

8. Nomenclature

Latin Letters

A	area	m^2
dx	volume-element dimension in *x-a*xis	m
H	irradiation onto a surface	W/m^2
I	intensity of radiation	$W/m^2 sr$
k	enclosure cell number in the *z*-axis	-
M	relatively very large number for DOM approximation	-
n	refractive index of a medium	-
$\hat{\mathbf{n}}$	normal direction to a surface	-
q	radiative heat flux per unit area	W/m^2
r	position vector	-
R	additional term for DOM complex geometry	-
S	DOM approximation	-
S	radiative source function	-
s	geometric path length	m
$\hat{\mathbf{s}}$	unit vector	-
T	temperature	K or °C
V	volume	m^3

Greek Symbols

α	absorptivity	-
γ	finite-difference weighting factor	-
η	*y*-axis DOM direction coordinate	-
κ	medium absorption coefficient	m^{-1}
μ	*z*-axis DOM direction coordinate	-
ν	frequency	s^{-1}
ξ	*x*-axis DOM direction coordinate	-
ρ	total hemispherical reflectivity	-
σ	Stefan-Boltzmann constant, 5.670×10^{-8}	$W/m^2 K^4$
ω	DOM ordinates weight	-
Ω	solid angle	sr
ε	total hemispherical emissivity	-

Subscripts

b	related to the blackbody
C	related to DOM numerator term
Cx	related to DOM numerator term, *x*-axis direction
P	related to DOM denominator term
P	related to a point *P*
Px	related to DOM denominator term, *x*-axis direction
s	related to the sensor surface
x	in *x*- direction
XE	downstream volume-element surface, *x*-axis
XR	upstream volume-element surface, *x*-axis
y	in *y*- direction
YR	upstream volume-element surface, *y*-axis
z	in *z*- direction
ZR	upstream volume-element surface, *z*-axis
w	wall

Superscripts

'	directional values

9. References

Almeida, J.S., 2000, “Measurement of Radiation in Complex Geometries and Comparison with Calculational Techniques, Ph.D. thesis, Loughborough University, Loughborough, United Kingdom

Brewster, M.Q., 1992, "Thermal Radiative Transfer and Properties", John Wiley & Sons, Inc., New York

Captec, 1999, "Radiant Heat Flux Sensors", Captec Enterprise, Villeneuve D'ascq, France

Carlson, B.G. and Lathrop, K. D., 1968, “Transport Theory - The Method of Discrete Ordinates”, Computing Methods in Reactor Physics, H. Greenspan, Gordon & Breach, New York, pp.165-266

Chai, J.C., Lee, H.S. and Patankar, S.V., 1993, “Treatment of Irregular Geometries Using a Cartesian-Coordinates-Based Discrete-Ordinates Method”, HTD - Vol. 244, Radiative Heat Transfer: Theory and Applic. - ASME, pp. 49-54

Chandrasekhar, S., 1960, "Radiative Transfer", Dover Publications, Inc., New York

Corlett, R.C., 1966, “Direct Monte Carlo Calculation of Radiative Heat Transfer in Vacuum”, Journal of Heat Transfer, pp. 376-382

Crosbie, A.L. and Schrenker, R.G., 1982, "Exact Expressions for Radiative Transfer in a Three-Dimensional Rectangular Geometry", Journal of Quantum Spectroscopy and Radiative Transfer, Vol. 28 (6), pp. 507-526

Fiveland, W.A., 1984, "Discrete-Ordinates Solutions of the Radiative Transport Equation for Rectangular Enclosures", Journal of Heat Transfer - Vol. 106, pp. 699-706

Fiveland, W.A., 1988, "Three-Dimensional Radiative Heat-Transfer Solutions by the Discrete-Ordinates Method", Journal of Thermophysics, Vol. 2(4), pp. 309-316

Lee, C.E., 1962, “The Discrete S_N Approximation to Transport Theory”, Technical Information Series - LA 2595 - Lawrence Livermore Laboratory, USA

Modest, M.F., 1993, "Radiative Heat Transfer", McGraw-Hill International Editions

Patankar, S.V., 1980, "Numerical Heat Transfer and Fluid Flow", Hemisphere Publishing Corporation, McGraw-Hill Book Company, Washington, U.S.A.

Sanchez, A. and Smith, T.F., 1992, “Surface Radiation Exchange for Two-Dimensional Rectangular Enclosures Using the Discrete-Ordinates Method”, Journal of Heat Transfer, Vol. 114, pp. 465-472

Selçuk, N. and Kayakol, N., 1997, “Evaluation of Discrete Ordinates Method for Radiative Transfer in Rectangular Furnaces”, Internat. Journal of Heat and Mass Transfer, Vol. 40(2), pp. 213-222

Siegel R. and Howell, J.R., 1992, “Thermal Radiation Heat Transfer”, Hemisphere Publishing Corporation, Washington, U.S.A.

Truelove, J.S., 1987, “Discrete-Ordinate Solutions of the Radiation Transport Equation”, Journal of Heat Transfer, Vol. 109, pp. 1048-1051